JOC The Journal of Organic Chemistry

pubs.acs.org/joc Article

Bacterial Biosynthetic P450 Enzyme $PikC_{D50N}$: A Potential Biocatalyst for the Preparation of Human Drug Metabolites

Jiawei Guo, Fengwei Li, Fangyuan Cheng, Li Ma, Xiaohui Liu, Pradeepraj Durairaj, Gang Zhang, Dandan Tang, Xiangtian Long, Wei Zhang, Lei Du, Xingwang Zhang,* and Shengying Li

Cite This: J. Org. Chem. 2021, 86, 14563−14571 Read Online

ACCESS | Metrics & More | Article Recommendations | Supporting Information

ABSTRACT: Human drug metabolites (HDMs) are important chemicals widely used in drug-related studies. However, acquiring these enzyme-derived and regio-/stereo-selectively modified compounds through chemical approaches is complicated. PikC is a biosynthetic P450 enzyme involved in pikromycin biosynthesis from the bacterium *Streptomyces venezuelae*. Here, we identify the mutant $PikC_{D50N}$ as a potential biocatalyst, with a broad substrate scope, diversified product profile, and high catalytic efficiency, for preparation of HDMs. Remarkably, $PikC_{D50N}$ can mediate the drug-metabolizing reactions using the low-cost H_2O_2 as a direct electron and oxygen donor.

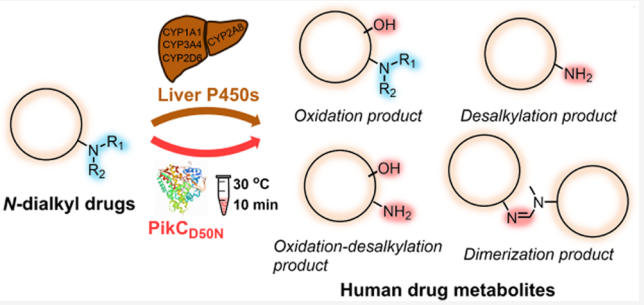

INTRODUCTION

Human drug metabolites (HDMs) are essential chemical standards for drug-related studies on pharmacology, pharmacokinetics, pharmacodynamics, and toxicology.[1] In the human body, these metabolites are predominantly produced by the catalysis of liver cytochrome P450 monooxygenases (P450s).[2] The P450-based drug metabolites not only change the stability, solubility, and bioavailability of the parent drugs but also play a crucial role in maintaining the biological activity, or, on the contrary, it may result in toxicity to the human body.[1] Therefore, stringent testing procedures have been developed to validate the bioactivity/toxicity of these metabolites in drug development.[1,3] In addition, due to the lack of related chemical standards, structural determination of HDMs in drug metabolism studies remains a challenging task.[4] Thus, the preparation of HDMs in pure form is indispensable for drug development. However, it is impractical to acquire the enzyme-derived HDMs from their parent drugs by chemical approaches, mainly due to the challenges in regio- and (or) stereoselectivity, and the total synthesis of HDMs is usually inefficient, cost-prohibitive, and eco-unfriendly.

Therefore, potential biocatalysts have long been expected for HDM preparation because human or mammalian P450s are difficult to be directly used owing to their membrane-bound nature, instability, dependency on expensive cofactor, and catalytic inefficiency.[5−7] To date, P450 BM3, a fatty acid hydroxylase discovered from *Bacillus megaterium*, has been studied as a prototype of the P450 catalyst to produce HDMs.[8] However, intensive protein engineering and/or directed evolution approaches are required to broaden the substrate scope of this bacterial P450.[9−12] Thus, a soluble P450 with innate substrate flexibility and a similar metabolite profile to that of human P450s would be a potential biocatalyst for HDM preparation.

PikC (CYP107L1) is a P450 enzyme from the pikromycin biosynthetic pathway in *Streptomyces venezuelae* and can be expressed well in *Escherichia coli*.[13] Its native function is to catalyze the hydroxylation of C10/C12 and C12/C14 against the 12- and 14-membered ring macrolides YC-17 and narbomycin, respectively (Figure 1).[13] An interesting "anchoring mechanism", in which the dimethylamino group is anchored to the acidic amino acid residues of PikC, for the substrate-PikC interaction was revealed through a detailed structural analysis.[14] In the previous studies, the substrate spectrum of PikC was successfully broadened by employing a "substrate engineering" strategy, where the natural derived or synthesized dimethylamino group was used as an artificial anchor to locate the unnatural substrate to the heme-iron center of PikC, according to its specific mechanism (Figure 1).[15−17]

Inspired by the substrate engineering strategy, in this study, we selected 19 human clinical drugs with different structure types and medicinal utilities, but all carrying the dialkylamino group to test the *in vitro* catalytic activity of PikC. The tested drugs include chlorpromazine (**1**), imipramine (**2**), chlorpro-

Received: June 14, 2021
Published: October 18, 2021

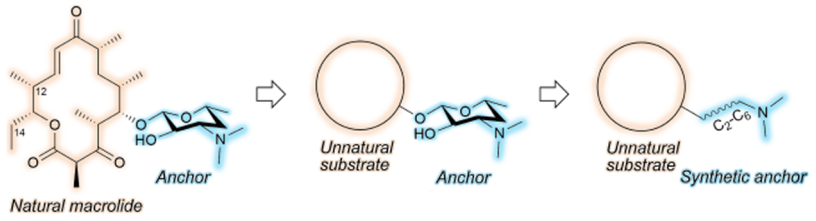

Figure 1. Substrate engineering strategy used for PikC.

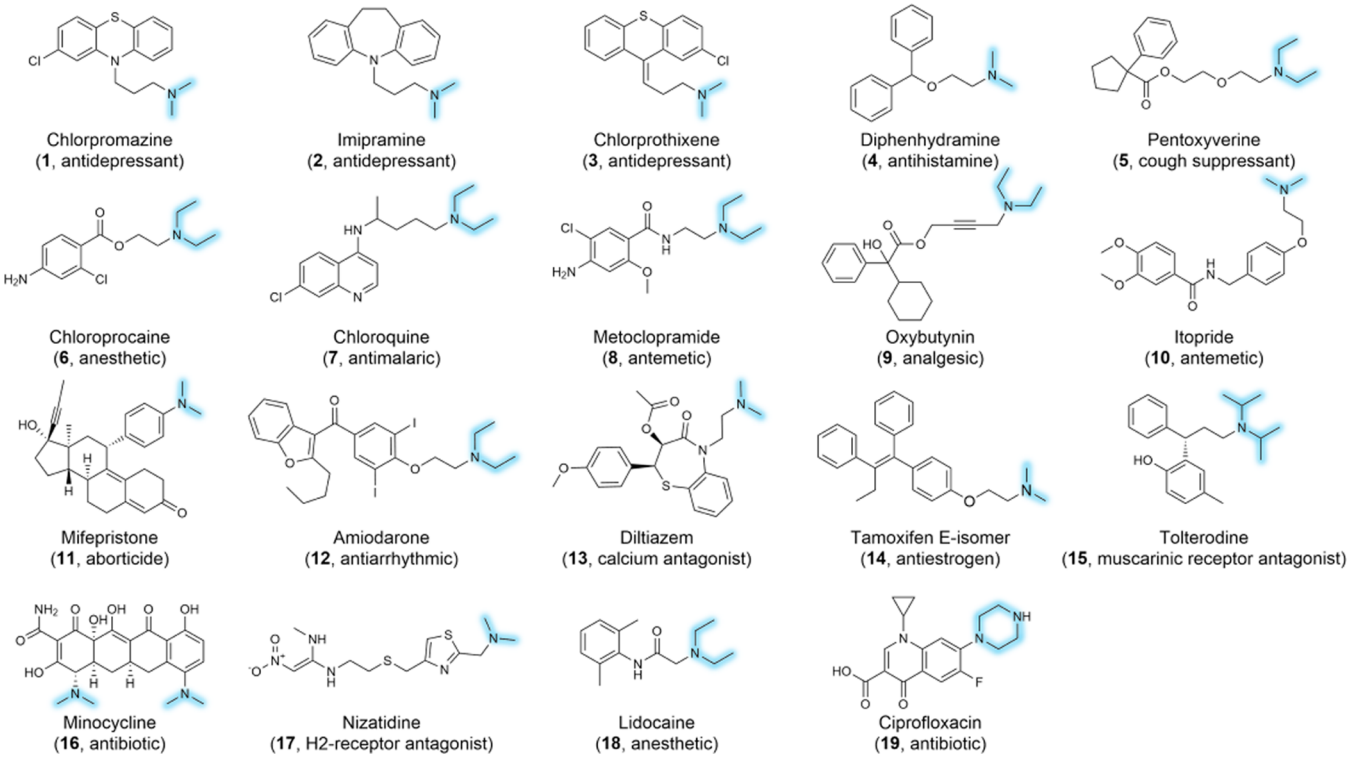

Figure 2. Chemical structures of the drugs used in this study (the dialkylamino groups are highlighted in blue and the clinical applications are indicated in brackets).

thixene (**3**), diphenhydramine (**4**), pentoxyverine (**5**), chloroprocaine (**6**), chloroquine (**7**), metoclopramide (**8**), oxybutynin (**9**), itopride (**10**), mifepristone (**11**), amiodarone (**12**), diltiazem (**13**), tamoxifen *E*-isomer (**14**), tolterodine (**15**), minocycline (**16**), nizatidine (**17**), lidocaine (**18**), and ciprofloxacin (**19**) (Figure 2).

RESULTS AND DISCUSSION

In the *in vitro* bioassays, the previously constructed mutant of PikC, $PikC_{D50N}$, whose catalytic activity was increased 4 times,[18] was used to react with **1**−**19**, with the *Synechococcus elongatus* PCC 7942 derived Fdx1499 and FdR0978 as redox partners (Figure S1).[19] Intriguingly, 15 out of the 19 tested drugs can be converted by $PikC_{D50N}$ into plenty of products with varying conversion rates, as shown in Table 1. Thereafter, we used a combination of methods including high-performance liquid chromatography−high-resolution mass spectrometry (HPLC-HRMS), gas chromatography (GC)-MS, HR-MS/MS, and nuclear magnetic resonance (NMR) to identify these metabolites (see Supporting Figures S2−S132). The results revealed that $PikC_{D50N}$ could act as a human P450 "mimicry" with the capacity of producing similar product profiles, including the main *N*-dealkylation and hydroxylation products (Table 1 and Figure 3).

Specifically, the *N*-alkyl-oxidized products, mainly N-dealkylation derivatives, were identified as the major products (Table 1 and Figure 3). In detail, $PikC_{D50N}$ preferentially oxidized **1**−**4**, **10**, **11**, **13**, and **14** to their corresponding *N*-demethylation and *N*-dedimethylation (except for **10**) products; **5**−**8** to the *N*-deethylation and the *N*-dediethylation (except for **5** and **8**) products; and **15** to the *N*-deisopropylation product. It is worth noting that, in the human body, the liver P450s also predominantly convert the *N*-alkyl-containing drugs into *N*-dealkylation products, making the resulting compounds more hydrophilic and to be readily excreted from the body (Table 1 and Figure 3).[20] Since the chemical synthesis of the *N*-dealkylation products of parent drugs via selective C−N bond cleavage is impracticable, the *N*-dealkylation functionality of $PikC_{D50N}$ significantly meets the demand for the preparation of *N*-dealkylation metabolites for the *N*-alkyl-carrying drugs.

Compared with the *N*-dealkylation reactions, monooxygenation toward the carbon skeleton is the dutiful function of $PikC_{D50N}$. As expected, a number of hydroxylated products were identified from the $PikC_{D50N}$-catalyzed reactions against

https://doi.org/10.1021/acs.joc.1c01407
J. Org. Chem. 2021, 86, 14563−14571

Table 1. Catalytic Properties of $PikC_{D50N}$ Compared with Those of the Related Human P450s

drug name	conversion rate (%)[a]	number of products[b]	reaction types of $PikC_{D50N}$	main human drug metabolizing P450s and the related reaction types
chlorpromazine (**1**)	95.5 ± 0.2	12	*N*-demethylation hydroxylation *S*-oxidation *N*-oxidation *N*-des-carbon-chain aldehydation dimerization	*N*-demethylation (CYP1A2)[21,22] hydroxylation(CYP2D6, CYP1A2)[21] *S*-oxidation (CYP1A2, CYP3A4)[21,22] *N*-oxidation (NI[c])[22] *N*-des-carbon-chain (NI[c])[23]
imipramine (**2**)	96.9 ± 1.9	11	*N*-demethylation hydroxylation	*N*-demethylation (CYP2D6)[24] hydroxylation (CYP1A2, CYP2C19, CYP3A4)[24]
chlorprothixene (**3**)	99.1 ± 0.4	5	*N*-demethylation *S*-oxidation	*N*-demethylation (NI[c])[25] *S*-oxidation (NI[c])[25]
diphenhydrmine (**4**)	78.5 ± 2.1	2	*N*-demethylation	*N*-demethylation (CYP2D6)[26,27]
pentoxyverine (**5**)	86.1 ± 4.4	5	*N*-deethylation hydroxylation	*N*-deethylation (NI[c])[28] hydroxylation (NI[c])[28]
chloroprocaine (**6**)	42.2 ± 6.7	2	*N*-deethylation	not reported
chloroquine (**7**)	39.4 ± 6.7	2	*N*-deethylation	*N*-deethylation (CYP2A8, CYP3A4/5)[27,29]
metoclopramide (**8**)	3.8 ± 1.5	1	*N*-deethylation	*N*-deethylation (CYP2D6)[4] hydroxylation (CYP2D6, CYP1A2)[4] nitro formation (CYP2D6, CYP1A2)[4]
oxybutynin (**9**)	100.0	5	hydroxylation	*N*-deethylation (CYP3A4, CYP3A5)[27,30]
itopride (**10**)	5.9 ± 3.4	1	*N*-demethylation	Not reported
mifepristone (**11**)	43.3 ± 3.8	3	*N*-demethylation hydroxylation	*N*-demethylation (CYP3A4, CYP3A5)[31] hydroxylation (CYP3A4)[31]
amiodarone (**12**)	71.4 ± 0.9	7	hydroxylation	*N*-deethylation (CYP1A1, CYP3A4)[27,32] hydroxylation (NI[c])[33]
diltiazem (**13**)	49.8 ± 6.7	2	*N*-demethylation	*N*-demethylation (CYP3A4, CYP2C8, CYP2C9)[27,34]
tamoxifen E-isomer (**14**)	72.0 ± 0.3	9	*N*-demethylation hydroxylation	*N*-demethylation (CYP2D6, CYP1A1, CYP3A4)[35] hydroxylation (CYP2B6, CYP2D6, CYP1B1)[35]
tolterodine (**15**)	60.0 ± 3.8	4	*N*-deisopropylation hydroxylation aldehydation successive oxidation	*N*-deisopropylation (CYP3A)[36] hydroxylation (CYP3A4, CYP2D6)[36] successive oxidation (NI[c])[36]

[a]The conversion rates are calculated from the decrease in substrate concentration quantified by fitting to related standard curves (Figure S133 and Table S2). [b]The products with yields <1% are omitted in this table. [c]NI indicates that the P450 member for producing the related HDM remains unidentified.

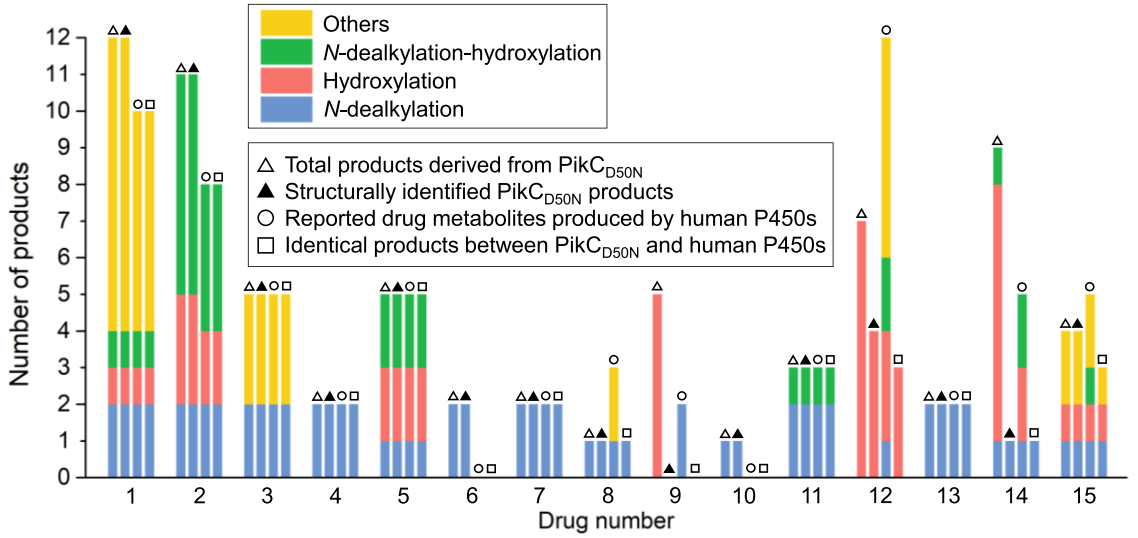

Figure 3. Comparisons between drug metabolites derived from $PikC_{D50N}$ and human liver P450s.

1, **2**, **5**, **9**, **11**, **12**, **14**, and **15** with different yields (Table 1 and Figure 3). In particular, multisite hydroxylation (dihydroxylation for **2**, **9**, **12**, and **14**, and trihydroxylation for **14**) and successive oxidation products (for **1** and **15**) were also formed in several reactions. In addition, as for **1**, **2**, **5**, **11**, and **14**, $PikC_{D50N}$ concurrently oxidized the *N*-dialkyl group and the carbon skeleton to yield the *N*-dealkylation-hydroxylation products. Apart from the major *N*-dealkylation and monooxygenation products, $PikC_{D50N}$ can also produce *S*-oxidation, *N*-oxidation, *N*-de-carbon-chain, and dimerization metabolites (Table 1 and the Supporting Figures).

Structural comparisons revealed that most of the identified products (45/55) were identical to HDMs derived from the human P450 (Figure 3). Specifically, for **1**, **2**, **6**, **10**, and **14**, the number of $PikC_{D50N}$-derived products exceeded that of the identified HDMs; for **3**, **4**, **5**, **7**, **11**, and **13**, the $PikC_{D50N}$-derived products overlap well with the identified HDMs (Figure 3). It was deduced that for **1**, **2**, **6**, and **10**, some trace HDMs may be neglected during drug metabolism studies due to the lack of chemical standards. Thus, in such a situation, $PikC_{D50N}$ can be used as a model to predict and produce the HDMs of the related drugs. Meanwhile, the number of $PikC_{D50N}$-derived products for **8**, **9**, **12**, and **14** is less than that of HDMs observed *in vivo*. Therefore, $PikC_{D50N}$ cannot modify all dialkylamino groups containing drugs into the related HDMs possibly due to the unfavorable structure size/type.

It is known that modified redox partners can change the product distribution of a P450-catalyzed reaction.[19] Thus, in

https://doi.org/10.1021/acs.joc.1c01407
J. Org. Chem. 2021, 86, 14563−14571

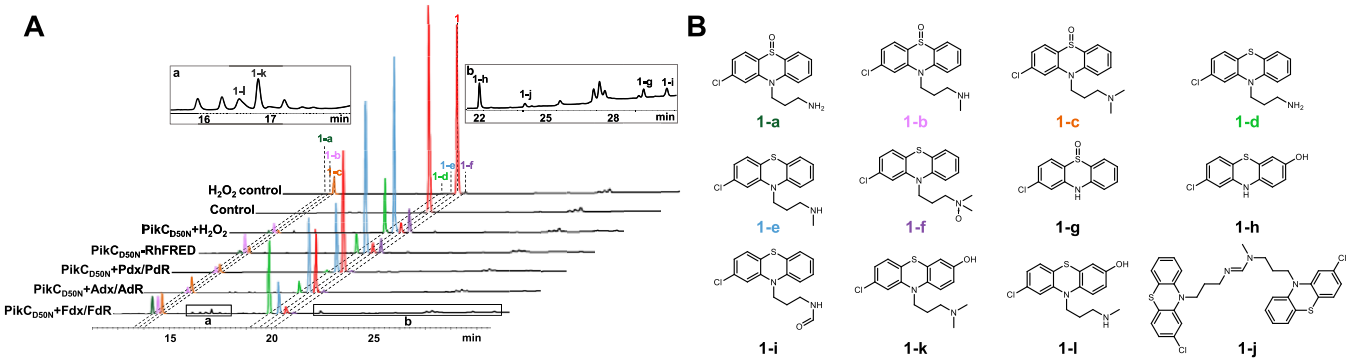

Figure 4. PikC$_{D50N}$-**1** reaction. (A) HPLC analyses (254 nm) of the 10 min incubation reaction of PikC$_{D50N}$-**1** supported by different redox partners or H_2O_2 (10 mM). Note: **1-c** could be spontaneously formed in the H_2O_2 control group under the oxidative condition. (B) Chemical structures of the products derived from the PikC$_{D50N}$-**1** reaction (the structure of **1-j** was assigned based on HR-ESI-MS/MS analysis).

Scheme 1. Putative Mechanism for the Formation of *N*-alkyl-Oxidized Products in the PikC$_{D50N}$-1 Reaction

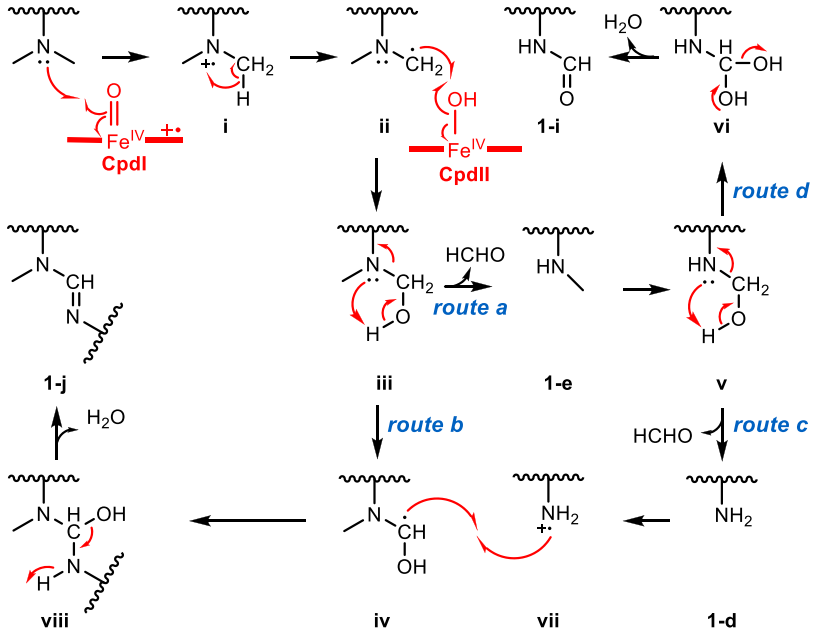

addition to Fdx1499/FdR0978, adrenodoxin (Adx)/adrenodoxin reductase (AdR) from *Bos taurus* and putidaredoxin (Pdx)/putidaredoxin reductase (PdR) from *Pseudomonas putida* were used to support the activities of PikC$_{D50N}$ (Figure S2). In addition, the previously constructed self-sufficient mutant PikC$_{D50N}$-RhFRED (Figures S1 and S135), a fused protein with the *Rhodococcus* sp. NCIMB 9784 derived reductase RhFRED, was also employed because it can skip the use of the complex redox−paterner system.[37] We chose **1** as a representative substrate because the PikC$_{D50N}$-**1** reaction has a high conversion rate (95.5%) and a diverse product profile (12 products). As expected, the results indicated that different redox partners considerably changed the product profiles of the PikC$_{D50N}$-**1** reaction, while Fdx1499/FdR0978 and PikC$_{D50N}$-RhFRED showed higher activities than the other two groups of redox partners (Figure 4). The different product profiles in the above reactions indicated that redox partners could be used as a "modulator" to prepare different drug metabolites. For example, the Adx/AdR and Pdx/PdR systems are suitable for the preparation of **1-e** because of the excellent product specificity. The self-sufficient PikC$_{D50N}$-RhFRED-catalyzed reaction could be used for generating **1-b**, **1-d**, **1-e**, and **1-f** as the major products. The Fdx1499/FdR0978 system may be useful for the preparation of the minor products (such as **1-a**, **1-h**, **1-g**, and **1-i**), which are formed only in trace amounts in other reactions (Figure 4).

Notably, the above conversions can be completed in 10 min at 30 °C, which demonstrates the high catalytic efficiency of PikC$_{D50N}$ toward the unnatural substrate **1**. In fact, the k_{cat}/K_m value of PikC$_{D50N}$ against **1** in the Fdx1499/FdR0978-supported reaction reached 1.59 ± 0.92 μM^{-1} min^{-1} (Figure S136), which is even higher than that for its native substrate YC-17 (0.24 μM^{-1} min^{-1}).[37]

Moreover, we investigated if PikC$_{D50N}$ can use H_2O_2 as a cofactor to drive the oxidative modifications of **1** to avoid the use of the redox partner proteins as well as the expensive cofactor NADPH. Interestingly, PikC$_{D50N}$ could efficiently use H_2O_2 (1−20 mM) to transform **1** into a broad spectrum of products (Figures 4A and S137). The capacity of using the low-cost H_2O_2 to mediate the above reactions with high conversion rates and great efficiency definitely demonstrated the application potential for PikC$_{D50N}$ in the large-scale preparation of drug metabolites.

https://doi.org/10.1021/acs.joc.1c01407
J. Org. Chem. 2021, 86, 14563−14571

To test the catalytic ability of $PikC_{D50N}$ at a preparative scale, 100 mg of **1** was incubated with the $PikC_{D50N}$–H_2O_2 system in a reaction volume of 100 mL. The HPLC analysis showed that both the substrate conversion rate and product profile (Figure S138) were similar to those in the analytical scale (100 μL) under the same P450 concentrations (2 μM). Upon product extraction and purification by preparative HPLC, 2.2 mg of **1-a**, 2.6 mg of **1-c**, 19.3 mg of **1-d**, 23.6 mg of **1-e**, and 4.4 mg of **1-f** were gained. To further prepare the minor products, the $PikC_{D50N}$–Fdx1499/FdR0978 system was employed to react with 200 mg of **1** in a 200 mL reaction. Likewise, the substrate conversion rate and product profile were also maintained at such a preparative scale (Figure S139), and another five products (**1-b** 4.2 mg; **1-g** 2.3 mg; **1-h** 5.5 mg; **1-i** 6.9 mg; **1-j** 0.9 mg) were purified. These results confirmed that $PikC_{D50N}$ can be applied in the preparation of HDMs.

To rationalize various types of reactions mediated by $PikC_{D50N}$ against **1**, we performed molecular docking studies using the crystal structure of $PikC_{D50N}$ (PDB ID: 3ZPI). The results showed that due to the large catalytic pocket of $PikC_{D50N}$,[14] compound **1** could adopt multiple binding conformations (Figure S140). Specifically, within the docked structure models, *N*-dimethyl was not captured as an anchor possibly due to the conformational flexibility of the connective aliphatic carbon chain; instead, they may readily approach the heme-iron center of $PikC_{D50N}$ because of the interattractive property of the amine group and iron, thus leading to *N*-oxidation as the major modification. We propose that this catalytic mode of action may be similar to that of the human P450s, and this should be the reason why they can produce similar product files. However, **16**–**19** could not be converted by $PikC_{D50N}$ likely due to their inappropriate structural size/shape and/or the inflexibility of their connective groups.

In addition, a catalytic mechanism for $PikC_{D50N}$ toward **1** was proposed to explain various types of reactions catalyzed by $PikC_{D50N}$ (Scheme 1). As has been investigated for human P450 3A4,[38,39] to start the *N*-oxidation reaction, compound I (CpdI; the reactive species of P450) of $PikC_{D50N}$ primarily abstracts a single electron from the lone pair of the amine to yield a cation radical (**i**), which could undergo an electron rearrangement to give the *Me*-radical (**ii**). Next, [HO$^{\bullet}$] rebound from compound II (CpdII) to **ii** forms the *Me*-hydroxylated product **iii**, which is unstable and can trigger a carbon–carbon bond cleavage reaction to yield the *N*-desmethyl product **1-e** (route a) before being oxidized in a second cycle to yield the species **iv** (route b). Then, $PikC_{D50N}$ hydroxylates **1-e** to form another unstable hydroxylated intermediate **v**. For **v**, it is speculated that it can either be spontaneously converted into **1-d** (route c) or hydroxylated for the second time to give **1-i** *via* the unstable geminal-diol intermediate **vi** (route d). The radical in **iv** could pair with the *N*-cation radical in **vii**, which can be formed *via* *N*-electron abstraction upon **1-d** and yield the dimer **1-j** after a further dehydration reaction in **viii**. When oxidation occurs at the core skeleton of **1**, the *S*-oxidation, *N*-des-carbon-chain, and hydroxylation products would be formed.

Furthermore, we tested the catalytic activity of $PikC_{D50N}$ toward six drugs without the dialkylamino group in their structures (Figure S141), including paclitaxel (**20**), coumarin (**21**), progesterone (**22**), vitamin D3 (**23**), pantoprazole (**24**), and mycophenolic acid (**25**). None of these drugs were metabolized by $PikC_{D50N}$ (Figures S142–S147), which is unsurprising because the dialkylamino group is essential for the substrate recognition of $PikC_{D50N}$ according to the previous "substrate engineering" studies of PikC (Figure 1).[15−17] We envision that this limitation could be overcome by more "enzyme engineering" efforts in future studies.[40,41]

CONCLUSIONS

The preparation of the site- and stereoselectively oxidized HDMs remains a challenging task. To address this issue, in this study, we identified a useful P450 enzyme $PikC_{D50N}$ for the preparation of HDMs in a cost-effective manner. Compared with the previously reported P450s used for HDM preparations, $PikC_{D50N}$ demonstrated its remarkable substrate flexibility by transforming 15 out of the 19 selected drugs into various oxidized products, and our product identification revealed that $PikC_{D50N}$ shows similar product profiles as human P450s. Structure comparisons revealed $PikC_{D50N}$ has a similar large and flexible substrate-binding pocket to that of the human P450 3A4, while BM3 carries a tubular catalytic pocket (Figure S148),[18,42,43] thus indicating $PikC_{D50N}$ to be an advantageous P450 biocatalyst for HDM preparation. In addition, this study will open the path to explore the novel catalytic properties of PikC and other biosynthetic P450s from microorganisms.

EXPERIMENTAL SECTION

Materials. All of the tested drugs were purchased from National Institutes for Food and Drug Control (Beijing, China) or Sinopharm Chemical Reagent Co., Ltd. (Shanghai, China). All antibiotics used in this study were obtained from Solarbio (Beijing, China). Organic solvents were purchased from Merck KGaA (Darmstadt, Germany). NADPH and IPTG were purchased from Aladdin (Shanghai, China). Ni-NTA SefinoseTM Resin (Settled Resin) for protein purification was acquired from Sangon Biotech (Shanghai, China). The FlexiRun premixed gel solution for SDS-PAGE was obtained from MDBio (Qingdao, China).

Analytical Methods. All HPLC analyses were carried out on a Thermo UltiMate 3000 instrument (Germering, Bavaria, Germany). The UV–vis absorbance measurements were conducted using a SpectraMax M2 plate reader. HR-LCMS and HR-MS/MS spectra were performed using a Triart C18 column (4.6 mm × 250 mm × 5 μM) (YMC Co., Ltd., Japan) on a Bruker Maxis UHR-TOF equipment. Nuclear magnetic resonance (NMR) spectra were recorded on a Bruker Avance III 600 MHz spectrometer, and NMR data were processed using MestReNova. Structural assignments were made with additional information from gCOSY, gHSQC, and gHMBC experiments. All GC-MS analyses were performed using a DB-5MS column (30 m × 0.25 mm × 0.25 μm) on a Thermo 01193K GC-MS instrument with the following temperature program: 80 °C for 1 min, 80–220 °C at 5 °C/min, 220 °C for 1 min, 220–290 °C at 3 °C/min, and 290 °C for 15 min.

Protein Expression and Purification. The expression strains of $PikC_{D50N}$, $PikC_{D50N}$-RhFERD, *Sel*Fdx1499/*Sel*FdR0978, Adx/AdR, Pdx/PdR, and glucose-6-phosphate dehydrogenase(GDH), for NADPH regeneration, were constructed during our previous studies.[14,19,37,44] All of the proteins were expressed in a 20 L fermentation cylinder (Shblbio, Shanghai, China). A colony of the expression strain was picked into 200 mL of LB Broth medium, containing 50 μg/mL of kanamycin, and grown at 37 °C, 220 rpm for 12 h. Then, the seed culture was used to inoculate into 15 L of Terrific broth (TB) medium containing 50 μg/mL of kanamycin at 37 °C, 400 rpm to grow for another 4–6 h. When OD_{600} reached 2.0–2.5, IPTG was added to the final concentration of 0.4 mM to induce protein expression, and the cells were grown for an additional 16–20 h at a lower temperature of 16 °C (to promote functional folding of the target protein). Subsequently, the cells were harvested by centrifugation (4000*g*; 10 min; 4 °C). Then, the collected cells were suspended in 500 mL of lysis buffer (50 mM NaH_2PO_4, 300 mM

https://doi.org/10.1021/acs.joc.1c01407
J. Org. Chem. 2021, 86, 14563−14571

NaCl, 10 mM imidazole, 10% glycerol, pH 8.0) and crushed by a high-pressure homogenizer (ATS, Shanghai, China) at 4 °C. After bacterial fragments were removed by centrifugation (10 000*g*; 60 min; 4 °C), 20 mL of Ni-NTA agarose was added into the supernatant to be incubated at 4 °C for 1h. The resin bound with His_6-tagged protein was loaded onto a gravity flow column, then washed with 2 L of wash buffer (50 mM NaH_2PO_4, 300 mM NaCl, 20 mM imidazole, 10% Glycerol, pH 8.0), and eluted with 50 mL of elution buffer (50 mM NaH_2PO_4, 300 mM NaCl, 250 mM imidazole, 10% glycerol, pH 8.0) to desorb the target protein. The solution was concentrated by a suitable size Amicon ultrafiltration tube (10 kD for Fdxs and GDH, 30 kD for $PikC_{D50N}$ and FdRs; Shanghai, China), and the buffer was then exchanged with desalting buffer (50 mM NaH_2PO_4, 100 mM NaCl 10% glycerol, pH 7.4) using a PD-10 desalting column (Beijing, China, GE Healthcare) to remove imidazole. Finally, the purified proteins were flash-frozen by liquid nitrogen and stored at −80 °C for later use.

Protein Concentration Analysis. The functional concentrations of P450 $PikC_{D50N}$ and $PikC_{D50N}$-RhFERD were measured from the CO-bound reduced difference spectrum by the extinction coefficient ($\epsilon_{450\text{-}490}$) of 91 000 M^{-1} cm^{-1} according to our previously reported procedure.[45] Other protein concentrations were measured based on *A280* recorded by using a Nanodrop (Thermo) equipment.

P450 Enzymatic Assay. The analytical scale reactions were carried out with a volume of 100 μL in a centrifuge tube, and the preparative scale reactions were performed with a volume of 100/200 mL in a conical flask. A typical reaction system contains 2 μM $PikC_{D50N}$, 200 μM substrate (preparative scale reactions was 3 mM), 20 μM *Sel*Fdx1499/10 μM *Sel*FdR0978 (20 μM Adx/10 μM AdR or 20 μM Pdx/10 μM PdR), and 2 mM NADPH in the reaction buffer (50 mM NaH_2PO_4, pH7.3, 1 mM EDTA, 0.2 mM dithioerythritol, and 10% glycerol). The reaction was incubated at 30 °C for 10 min or longer time. The $PikC_{D50N}$-RhFRED reaction system contains 2 μM $PikC_{D50N}$-RhFRED, 200 μM compound **1**, and 2 mM NADPH. The $PikC_{D50N}$-H_2O_2 reaction system contains 2 μM $PikC_{D50N}$, 200 μM compound **1**, and 100 μM−20 mM H_2O_2. Boiled $PikC_{D50N}$ was used in the negative controls. For analytical reactions, 100 μL of methanol was added to quench the reaction and to precipitate proteins, and the supernatant was subjected to HPLC and LC-MS analysis after high-speed centrifugation (10 000*g*; 10 min). For the preparative scale reactions, ethyl acetate was used for product extraction.

The reaction samples were analyzed by HPLC under the linear gradient mobile phase of 10% (v/v) acetonitrile/H_2O to 80% (v/v) (for **1**, **2**, **4**, **6**−**8**, **10**, **13**, **16**−**22**, **24**, and **25**), 20% (v/v) to 70% (v/v) acetonitrile/H_2O (for **5**, **9**, **12**, **14**, and **15**), 20% (v/v) acetonitrile/H_2O to 60% (v/v) acetonitrile/H_2O (for **3**), or 30% (v/v) acetonitrile/H_2O to 80% (for **11**), over 30 min at a flow rate of 1 mL/min. The reaction sample of **23** were analyzed under an isocratic mobile phase of 95% (v/v) methanol/H_2O for 30 min at a flow rate of 1 mL/min.

Product Identification. The enzymatic products were first subjected to HPLC-HR-MS to identify the metabolite types, such as dealkylation, hydroxylation, and successive oxidation. As for the dealkylation products, we used HR-MS/MS analysis to confirm their structures. For the hydroxylation or other types of metabolites, we preferred to use GC-MS (EI source) to identify their structures by comparing them with the MS fragments in the database; otherwise, we identified the remaining products by HR-MS/MS fragmental comparisons (with reported data) or direct fragmental analysis. Especially, the products of **1** were further confirmed by NMR analysis.

Preparation of Standard Curves for 15 Drugs. Standard solutions of the **1**−**15** were prepared in the concentrations of 50, 100, 150, 200, and 250 μM in the mixed solution of methanol and reaction buffer (volume ratio = 1:1). Then, the solutions were performed on HPLC under the same condition of related drugs. The specific substrate peak area of various concentrations for these substrates was recorded and used for the preparation of standard curves according to the Lambert−Beer law. The concentrations of the residual substrates in the enzymatic reactions were quantified by fitting to the standard curves.

Preparation of Enzymatic Products of 1. One hundred milliliters of the reaction mixture of the $PikC_{D50N}$-H_2O_2 system and 200 mL of the reaction mixture of the $PikC_{D50N}$-Fdx/FdR system were extracted with an equal volume of ethyl acetate by vortex mixing, each for two times. The organic phase was concentrated *in vacuum*. The gained extracts were then subjected to a semipreparative HPLC system using YMC-Pack Pro C18 (10 mm × 250 mm × 5 μM) under a linear mobile phase gradient ranging from 20% (v/v) acetonitrile/H_2O to 80% (v/v) acetonitrile/H_2O over 40 min at a flow rate of 2.5 mL/min.

Steady-State Kinetic Analysis of $PikC_{D50N}$ Toward 1. One hundred fifty nanomolar $PikC_{D50N}$, 10 μM *Sel*Fdx1499, 5 μM *Sel*FdR0978, and 10−200 μM **1** was pre-incubated in a total volume of 400 μL at 30 °C for 5 min. Then, the reaction was initiated by adding 2 μL of 100 mM NADPH. Thereafter, 100 μL of the mixture was immediately (∼0 s) taken out to thoroughly mix with 100 μL of methanol to quench the reaction, and such a procedure was repeated two times at 20 s and 40 s. After high-speed centrifugation (12 000 *g*; 10 min), the supernatant was subjected to HPLC analysis. The HPLC conditions were as follows: a linear gradient mobile phase ranging from 10% (v/v) acetonitrile/H_2O to 65.2% (v/v) acetonitrile/H_2O over 16 min at a flow rate of 1 mL/min and using a UV wavelength of 254 nm. The initial velocity of the substrate consumption was deduced from the decreased area under the curve (AUC) of specific substrate peaks. Finally, the data from duplicate experiments were fit to the Michaelis−Menten equation.

Molecular Docking. The 3D structure of $PikC_{D50N}$ (PDB ID: 3ZPI) was obtained from the protein bank in RCSB. The molecular structure of compound **1** was generated using Chembio3D Ultra 11.0 followed by energy minimization. The AutoDock 4.2[46] program equipped with ADT was used to perform the automated molecular docking. All side chains were set as rigid body and grid spacing was set to 0.5 Å. Other parameters retained their default values. The top 30 lowest energy docking poses of $PikC_{D50N}$ from 2 500 000 searching results were chosen. The docking models were analyzed and represented using ADT and pymol (http://www.pymol.org).

NMR Data of 1-c, 1-d, 1-f, 1-g, 1-h, and 1-i. ***1-c***.[47] White amorphous solid; ^1H NMR (600 MHz, CD_3CN): δ 7.93 (dd, *J* = 7.7, 1.5 Hz, 1H), 7.89 (d, *J* = 8.2 Hz, 1H), 7.72 (t, *J* = 2.0 Hz, 1H), 7.71−7.68 (m, 1H), 7.66 (d, *J* = 8.1 Hz, 1H), 7.34−7.30 (m, 1H), 7.27 (dd, *J* = 8.2, 1.8 Hz, 1H), 4.41−4.36 (m, 2H), 2.76−2.72 (m, 2H), 2.40 (s, 6H), 2.14−2.07 (m, 2H). $^{13}C\{^1H\}$ NMR (151 MHz, CD_3CN): δ 140.4, 139.3, 138.8, 134.0, 133.2, 131.7, 126.5, 125.0, 123.4, 122.8, 117.9, 117.6, 55.6, 45.8, 44.2, 23.6; HRMS (ESI) calcd for $C_{17}H_{19}ClN_2OS$ $[M + H]^+$ 335.0979, found 335.0981.

1-d.[48] White amorphous solid; ^1H NMR (600 MHz, CD_3OD): δ 7.26−7.22 (m, 1H), 7.17 (dd, *J* = 7.7, 1.4 Hz, 1H), 7.13 (d, *J* = 8.2 Hz, 1H), 7.06 (s, 1H), 7.05 (d, *J* = 2.1 Hz, 1H), 7.00 (dd, *J* = 7.6, 1.0 Hz, 1H), 6.98 (dd, *J* = 8.2, 2.1 Hz, 1H), 4.06 (t, *J* = 6.4 Hz, 2H), 3.05−2.98 (m, 2H), 2.15−2.07 (m, 2H). $^{13}C\{^1H\}$ NMR (DEPT-Q) (151 MHz, CD_3OD): δ 129.1, 128.7, 128.5, 124.4, 123.7, 117.3, 117.1, 45.0, 38.4, 26.0; HRMS (ESI) calcd for $C_{15}H_{15}ClN_2S$ $[M + H]^+$ 291.0717, found 291.0714.

1-f.[22] White amorphous solid; ^1H NMR (600 MHz, CD_3CN): δ 7.25−7.22 (m, 1H), 7.18 (dd, *J* = 7.7, 1.3 Hz, 1H), 7.12 (d, *J* = 8.2 Hz, 1H), 7.02 (d, *J* = 1.6 Hz, 1H), 7.00 (d, *J* = 8.6 Hz, 1H), 7.01−6.98 (m, 1H), 6.98 (dd, *J* = 8.2, 1.9 Hz, 1H), 3.99 (t, *J* = 6.7 Hz, 2H), 3.50−3.45 (m, 2H), 3.15 (s, 6H), 2.22 (dd, *J* = 15.0, 7.3 Hz, 2H). $^{13}C\{^1H\}$ NMR (DEPT-Q) (151 MHz, CD_3CN): δ 128.2, 127.9, 127.6, 123.5, 122.7, 116.5, 116.3, 67.0, 56.4, 43.9, 20.6; HRMS (ESI) calcd for $C_{17}H_{19}ClN_2OS$ $[M + H]^+$ 335.0979, found 335.0975.

1-g.[23] Purple amorphous solid; ^1H NMR (600 MHz, CD_3OD): δ 7.94 (d, *J* = 1.3 Hz, 1H), 7.92 (d, *J* = 8.4 Hz, 1H), 7.66 (ddd, *J* = 8.5, 7.3, 1.4 Hz, 1H), 7.40 (d, *J* = 1.9 Hz, 1H), 7.39 (d, *J* = 8.2 Hz, 1H), 7.30−7.26 (m, 1H), 7.23 (dd, *J* = 8.4, 2.0 Hz, 1H). $^{13}C\{^1H\}$ NMR (DEPT-Q) (151 MHz, CD_3OD): δ 134.7, 134.0, 132.2, 123.4, 123.0, 118.2, 117.5; HRMS (ESI) calcd for $C_{12}H_8ClNOS$ $[M + H]^+$ 250.0088, found 250.0089.

1-h.[23] Purple amorphous solid; ^1H NMR (600 MHz, CD_3OD): δ 6.80 (d, *J* = 8.2 Hz, 1H), 6.67 (dd, *J* = 8.2, 2.0 Hz, 1H), 6.59 (d, *J* =

https://doi.org/10.1021/acs.joc.1c01407
J. Org. Chem. 2021, 86, 14563−14571

2.1 Hz, 1H), 6.48 (d, J = 8.5 Hz, 1H), 6.43 (dd, J = 8.5, 2.6 Hz, 1H), 6.37 (d, J = 2.6 Hz, 1H). $^{13}C\{^1H\}$ NMR (DEPT-Q) (151 MHz, CD_3OD): δ 128.1, 121.7, 116.2, 115.1, 114.6, 114.0; HRMS (ESI) calcd for $C_{12}H_8ClNOS$ $[M + H]^+$ 250.0089, found 250.0089.

1-i.[49] White amorphous solid; ^1H NMR (600 MHz, CD_3OD): δ 7.99 (s, 1H), 7.22−7.18 (m, 1H), 7.14−7.12 (m, 1H), 7.09−7.06 (m, 1H), 7.02−6.99 (m, 1H), 6.98 (d, J = 2.0 Hz, 1H), 6.96 (td, J = 7.5, 0.9 Hz, 1H), 6.93 (dt, J = 8.1, 2.1 Hz, 1H), 3.98−3.92 (m, 2H), 3.34−3.31 (m, 2H), 2.00−1.93 (m, 2H). $^{13}C\{^1H\}$ NMR (151 MHz, CD_3OD): δ 163.9, 129.0, 128.7, 128.4, 124.2, 123.4, 117.3, 117.0, 45.7, 36.6, 27.6; HRMS (ESI) calcd for $C_{16}H_{15}ClN_2OS$ $[M + H]^+$ 319.0666, found 319.0661.

The HR-MS, HR-MS/MS, and GC−MS data for the remaining products are given in the related figures and tables in the Supporting Information.

■ ASSOCIATED CONTENT

Supporting Information

The Supporting Information is available free of charge at https://pubs.acs.org/doi/10.1021/acs.joc.1c01407.

Enzymatic reaction schemes, HR-MS, HR-MS/MS, and GC-MS characterization data and NMR spectra of enzymatic products. The Supporting Information is available free of charge on the ACS Publications website (PDF)

■ AUTHOR INFORMATION

Corresponding Author

Xingwang Zhang − *State Key Laboratory of Microbial Technology, Shandong University, Qingdao, Shandong 266237, China;* orcid.org/0000-0003-1346-1183; Email: zhangxingwang@sdu.edu.cn

Authors

Jiawei Guo − *State Key Laboratory of Microbial Technology, Shandong University, Qingdao, Shandong 266237, China; Laboratory for Marine Biology and Biotechnology, Qingdao National Laboratory for Marine Science and Technology, Qingdao, Shandong 266237, China*

Fengwei Li − *State Key Laboratory of Microbial Technology, Shandong University, Qingdao, Shandong 266237, China*

Fangyuan Cheng − *State Key Laboratory of Microbial Technology, Shandong University, Qingdao, Shandong 266237, China*

Li Ma − *State Key Laboratory of Microbial Technology, Shandong University, Qingdao, Shandong 266237, China*

Xiaohui Liu − *State Key Laboratory of Microbial Technology, Shandong University, Qingdao, Shandong 266237, China*

Pradeepraj Durairaj − *State Key Laboratory of Microbial Technology, Shandong University, Qingdao, Shandong 266237, China*

Gang Zhang − *Fujian Universities and Colleges Engineering Research Center of Marine Biopharmaceutical Resources, Xiamen Medical College, Xiamen, Fujian 361023, China*

Dandan Tang − *State Key Laboratory of Microbial Technology, Shandong University, Qingdao, Shandong 266237, China*

Xiangtian Long − *Tianjin Hankang Pharmaceutical Biotechnology Co. Ltd., Tianjin 300409, China*

Wei Zhang − *State Key Laboratory of Microbial Technology, Shandong University, Qingdao, Shandong 266237, China;* orcid.org/0000-0001-9459-680X

Lei Du − *State Key Laboratory of Microbial Technology, Shandong University, Qingdao, Shandong 266237, China;* orcid.org/0000-0003-2245-7100

Shengying Li − *State Key Laboratory of Microbial Technology, Shandong University, Qingdao, Shandong 266237, China; Laboratory for Marine Biology and Biotechnology, Qingdao National Laboratory for Marine Science and Technology, Qingdao, Shandong 266237, China*

Complete contact information is available at: https://pubs.acs.org/10.1021/acs.joc.1c01407

Notes

The authors declare no competing financial interest.

■ ACKNOWLEDGMENTS

This work was supported by the National Key Research and Development Program of China (2019YFA0905100), the National Natural Science Foundation of China (32000039 and 32025001), the Fundamental Research Fund of Shandong University (2019GN031 and 2019GN030), the Laboratory for Marine Drugs and Bioproducts of Pilot National Laboratory for Marine Science and Technology (Qingdao) (LMDBKF-2019-01), and the Fujian Province Universities and Colleges Technology and Engineering Center for Marine Biomedical Resource, Xiamen Medical College (XMMC-MBS-201904). We thank Jingyao Qu, Jing Zhu, Zhifeng Li, and Haiyan Sui from the State Key Laboratory of Microbial Technology of Shandong University for their help in LC-MS, GC-MS, and NMR analyses.

■ REFERENCES

(1) Atrakchi, A. H. Interpretation and considerations on the safety evaluation of human drug metabolites. *Chem. Res. Toxicol.* **2009**, *22*, 1217−1220.

(2) Guengerich, F. P.; Waterman, M. R.; Egli, M. Recent structural insights into cytochrome P450 function. *Trends Pharmacol. Sci.* **2016**, *37*, 625−640.

(3) Guengerich, F. P. Introduction: Human metabolites in safety testing (MIST) issue. *Chem. Res. Toxicol* **2009**, *22*, 237−238.

(4) Livezey, M. R.; Briggs, E. D.; Bolles, A. K.; Nagy, L. D.; Fujiwara, R.; Furge, L. L. Metoclopramide is metabolized by CYP2D6 and is a reversible inhibitor, but not inactivator, of CYP2D6. *Xenobiotica* **2014**, *44*, 309−319.

(5) Stepan, A. F.; Tran, T. P.; Helal, C. J.; Brown, M. S.; Chang, C.; O'Connor, R. E.; De Vivo, M.; Doran, S. D.; Fisher, E. L.; et al. Late-stage microsomal oxidation reduces drug-drug interaction and identifies phosphodiesterase 2A inhibitor PF-06815189. *ACS Med. Chem. Lett.* **2018**, 68−72.

(6) O'Reilly, E.; Kohler, V.; Flitsch, S. L.; Turner, N. J. Cytochromes P450 as useful biocatalysts: addressing the limitations. *Chem. Commun.* **2011**, *47*, 2490−2501.

(7) Gonzalez, F. J. Human cytochromes P450: problems and prospects. *Trends Pharmacol. Sci.* **1992**, *13*, 346−352.

(8) Di Nardo, G.; Gilardi, G. Optimization of the bacterial cytochrome P450 BM3 system for the production of human drug metabolites. *Int. J. Mol. Sci.* **2012**, *13*, 15901−15924.

(9) Di Nardo, G.; Fantuzzi, A.; Sideri, A.; Panicco, P.; Sassone, C.; Giunta, C.; Gilardi, G. Wild-type CYP102A1 as a biocatalyst: turnover of drugs usually metabolised by human liver enzymes. *JBIC, J. Biol. Inorg. Chem.* **2007**, *12*, 313−323.

(10) Kim, D. H.; Ahn, T.; Jung, H. C.; Pan, J. G.; Yun, C. H. Generation of the human metabolite piceatannol from the anticancer-preventive agent resveratrol by bacterial cytochrome P450 BM3. *Drug Metab. Dispos.* **2009**, *37*, 932−936.

(11) Sawayama, A. M.; Chen, M. M. Y.; Kulanthaivel, P.; Kuo, M. S.; Hemmerle, H.; Arnold, F. H. A panel of cytochrome P450 BM3 variants to produce drug metabolites and diversify lead compounds. *Chem. - Eur. J.* **2009**, *15*, 11723−11729.
(12) Rentmeister, A.; Brown, T. R.; Snow, C. D.; Carbone, M. N.; Arnold, F. H. Engineered bacterial mimics of human drug metabolizing enzyme CYP2C9. *ChemCatChem* **2011**, *3*, 1065−1071.
(13) Xue, Y.; Wilson, D.; Zhao, L. S.; Liu, H.-W.; Sherman, D. H. Hydroxylation of macrolactones YC-17 and narbomycin is mediated by the PikC-encoded cytochrome P450 in *Streptomyces venezuelae*. *Chem. Biol.* **1998**, *5*, 661−667.
(14) Sherman, D. H.; Li, S.; Yermalitskaya, L. V.; Kim, Y.; Smith, J. A.; Waterman, M. R.; Podust, L. M. The structural basis for substrate anchoring, active site selectivity, and product formation by P450 PikC from *Streptomyces venezuelae*. *J. Biol. Chem.* **2006**, *281*, 26289−26297.
(15) Li, S. Y.; Chaulagain, M. R.; Knauff, A. R.; Podust, L. M.; Montgomery, J.; Sherman, D. H. Selective oxidation of carbolide C-H bonds by an engineered macrolide P450 mono-oxygenase. *Proc. Natl. Acad. Sci. U.S.A.* **2009**, *106*, 18463−18468.
(16) Negretti, S.; Narayan, A. R.; Chiou, K. C.; Kells, P. M.; Stachowski, J. L.; Hansen, D. A.; Podust, L. M.; Montgomery, J.; Sherman, D. H. Directing group-controlled regioselectivity in an enzymatic C-H bond oxygenation. *J. Am. Chem. Soc.* **2014**, *136*, 4901−4904.
(17) Narayan, A. R.; Jimenez-Oses, G.; Liu, P.; Negretti, S.; Zhao, W.; Gilbert, M. M.; Ramabhadran, R. O.; Yang, Y. F.; Furan, L. R.; Li, Z.; Podust, L. M.; Montgomery, J.; Houk, K. N.; Sherman, D. H. Enzymatic hydroxylation of an unactivated methylene C-H bond guided by molecular dynamics simulations. *Nat. Chem.* **2015**, *7*, 653−660.
(18) Li, S.; Ouellet, H.; Sherman, D. H.; Podust, L. M. Analysis of transient and catalytic desosamine-binding pockets in cytochrome P-450 PikC from *Streptomyces venezuelae*. *J. Biol. Chem.* **2009**, *284*, 5723−5730.
(19) Zhang, W.; Du, L.; Li, F.; Zhang, X.; Qu, Z.; Han, L.; Li, Z.; Sun, J.; Qi, F.; Yao, Q.; Sun, Y.; Geng, C.; Li, S. Mechanistic insights into interactions between bacterial class I P450 enzymes and redox partners. *ACS Catal.* **2018**, *8*, 9992−10003.
(20) Dang, N. L.; Hughes, T. B.; Miller, G. P.; Swamidass, J. Computationally assessing the bioactivation of drugs by N-dealkylation. *Chem. Res. Toxicol.* **2018**, *31*, 68−80.
(21) Wójcikowski, J.; Boksa, J.; Daniel, W. A. Main contribution of the cytochrome P450 isoenzyme 1A2 (CYP1A2) to N-demethylation and 5-sulfoxidation of the phenothiazine neuroleptic chlorpromazine in human liver-A comparison with other phenothiazines. *Biochem. Pharmacol.* **2010**, *80*, 1252−1259.
(22) Fishman, V.; Heaton, A.; Goldenberg, H. Metabolism of chlorpromazine. III. Isolation and identification of chlorpromazine-N-oxide. *Exp. Biol. Med.* **1962**, *109*, 548−552.
(23) Forrest, I.; Green, D.; Serra, M.; Chao, F.; Loeffler, K. Chlorpromazine excretion: II. Improved TLC procedures for fractionating the urinary drug content into chemical subgroups of CPZ metabolites. *Commun. Psychopharmacol.* **1978**, *2*, 131−138.
(24) Brøsen, K.; Skjelbo, E.; Nielsen, K. K. Imipramine: A model drug for P450 research. *Methods Enzymol.* **1996**, *272*, 177−186.
(25) Christensen, H. Chlorprothixene and its metabolites in blood, liver and urine from fatal poisoning. *Acta Pharmacol. Toxicol.* **1974**, *34*, 16−26.
(26) Akutsu, T.; Kobayashi, K.; Sakurada, K.; Ikegaya, H.; Furihata, T.; Chiba, K. Identification of human cytochrome p450 isozymes involved in diphenhydramine N-demethylation. *Drug Metab. Dispos.* **2007**, *35*, 72−78.
(27) Ram, N.; Kalász, H.; Adeghate, E.; Darvas, F.; Hashemi, F.; Tekes, K. Medicinal chemistry of drugs with active metabolites (N-, O-, and S-desalkylation and some specific oxidative alterations). *Curr. Med. Chem.* **2012**, *19*, 5683−5704.
(28) Westphal, F.; Junge, T.; Radunz, L.; Stegk, J.; Rochholz, G. Characterization of pentoxyverine metabolites in urine using GC/MS after intoxication with Silomat cough drops. *Forensic Sci. Int.* **2012**, *215*, 124−135.
(29) Kim, K. A.; Park, J. Y.; Lee, J. S.; Lim, S. Cytochrome P4502C8 and CYP3A4/5 are involved in chloroquine metabolism in human liver microsomes. *Arch Pharm. Res.* **2003**, *26*, 631−637.
(30) Mizushima, H.; Takanaka, K.; Abe, K.; Fukazawa, I.; Ishizuka, H. Stereoselective pharmacokinetics of oxybutynin and N-desethyloxybutynin *in vitro* and *in vivo*. *Xenobiotica* **2007**, *37*, 59−73.
(31) Khan, K. K.; He, Y. Q.; Correia, M. A.; Halpert, J. R. Differential oxidation of mifepristone by cytochromes P450 3A4 and 3A5: Selective inactivation of P450 3A4. *Drug Metab. Dispos.* **2002**, *30*, 985−990.
(32) Elsherbiny, M. E.; El-Kadi, A. O. S.; Brocks, D. R. The metabolism of amiodarone by various CYP isoenzymes of human and rat, and the inhibitory influence of ketoconazole. *J. Pharm. Pharm. Sci.* **2008**, *11*, 147−159.
(33) Ramesh Varkhede, N.; Jhajra, S.; Suresh Ahire, D.; Singh, S. Metabolite identification studies on amiodarone in *in vitro* (rat liver microsomes, rat and human liver S9 fractions) and *in vivo* (rat feces, urine, plasma) matrices by using liquid chromatography with high-resolution mass spectrometry and multiple-stage mass spectrometry: Characterization of the diquinone metabolite supposedly responsible for the drug's hepatotoxicity. *Rapid Commun. Mass Spectrom.* **2014**, *28*, 311−331.
(34) Sutton, D.; Butler, A. M.; Nadin, L.; Murray, M. Role of CYP3A4 in human hepatic diltiazem N-demethylation: Inhibition of CYP3A4 activity by oxidized diltiazem metabolites. *J. Pharmacol. Exp. Ther.* **1997**, *282*, 294−300.
(35) Crewe, H. K.; Notley, L. M.; Wunsch, R. M.; Lennard, M. S.; Gillam, E. M. Disposition, Metabolism of tamoxifen by recombinant human cytochrome P450 enzymes: formation of the 4-hydroxy, 4′-hydroxy and N-desmethyl metabolites and isomerization oftrans-4-hydroxytamoxifen. *Drug Metab. Dispos.* **2002**, *30*, 869−874.
(36) Ananchenko, G.; Novakovic, J. Tolterodine Tartrate. *Profiles Drug Subst., Excipients, Relat. Methodol.* **2017**, *42*, 339−403.
(37) Li, S. Y.; Podust, L. M.; Sherman, D. H. Engineering and analysis of a self-sufficient biosynthetic cytochrome P450 PikC fused to the RhFRED reductase domain. *J. Am. Chem. Soc.* **2007**, *129*, 12940−12941.
(38) Rydberg, P.; Jorgensen, M. S.; Jacobsen, T. A.; Jacobsen, A. M.; Madsen, K. G.; Olsen, L. Nitrogen Inversion Barriers Affect the N-Oxidation of Tertiary Alkylamines by Cytochromes P450. *Angew. Chem., Int. Ed.* **2013**, *52*, 993−997.
(39) Roberts, K. M.; Jones, J. P. Anilinic N-Oxides Support Cytochrome P450-Mediated N-Dealkylation through Hydrogen-Atom Transfer. *Chem. - Eur. J.* **2010**, *16*, 8096−8107.
(40) Acevedo-Rocha, C. G.; Gamble, C. G.; Lonsdale, R.; Li, A.; Nett, N.; Hoebenreich, S.; Lingnau, J. B.; Wirtz, C.; Fares, C.; Hinrichs, H.; Deege, A.; Mulholland, A. J.; Nov, Y.; Leys, D.; McLean, K. J.; Munro, A. W.; Reetz, M. T. P450-Catalyzed Regio- and Diastereoselective Steroid Hydroxylation: Efficient Directed Evolution Enabled by Mutability Landscaping. *ACS Catal.* **2018**, *8*, 3395−3410.
(41) Acevedo-Rocha, C. G.; Li, A.; D'Amore, L.; Hoebenreich, S.; Sanchis, J.; Lubrano, P.; Ferla, M. P.; Garcia-Borras, M.; Osuna, S.; Reetz, M. T. Pervasive cooperative mutational effects on multiple catalytic enzyme traits emerge via long-range conformational dynamics. *Nat. Commun.* **2021**, *12*, No. 1621.
(42) Haines, D. C.; Tomchick, D. R.; Machius, M.; Peterson, J. A. Pivotal role of water in the mechanism of P450BM-3. *Biochemistry* **2001**, *40*, 13456−13465.
(43) Ekroos, M.; Sjogren, T. Structural basis for ligand promiscuity in cytochrome P450 3A4. *Proc. Natl. Acad. Sci. U.S.A.* **2006**, *103*, 13682−13687.
(44) Ma, L.; Du, L.; Chen, H.; Sun, Y.; Huang, S.; Zheng, X.; Kim, E. S.; Li, S. Reconstitution of the *In Vitro* Activity of the Cyclosporine-Specific P450 Hydroxylase from *Sebekia benihana* and Development of a Heterologous Whole-Cell Biotransformation System. *Appl. Environ. Microbiol.* **2015**, *81*, 6268−6275.

https://doi.org/10.1021/acs.joc.1c01407
J. Org. Chem. 2021, 86, 14563−14571

(45) Sato, R. Cytochrome-P-450 - an Inconspicuous Start - a Citation-Classic Commentary on the Carbon Monoxide-Binding Pigment of Liver-Microsomes. 1. Evidence for Its Hemoprotein Nature. *Cc/Life Sci.* **1991**, 9.
(46) Morris, G. M.; Huey, R.; Lindstrom, W.; Sanner, M. F.; Belew, R. K.; Goodsell, D. S.; Olson, A. J. AutoDock4 and AutoDockTools4: Automated docking with selective receptor flexibility. *J. Comput. Chem.* **2009**, *30*, 2785−2791.
(47) Staiger, D. B.; Warren, R. J.; Zarembo, J. E.; Post, A.; Anderson, E. L. 13C NMR spectral analysis of chlorpromazine, chlorpromazine sulfoxide and related models. *J. Heterocycl. Chem.* **1981**, *18*, 101−103.
(48) Beckett, A.; Beaven, M.; Robinson, A. Metabolism of chlorpromazine in humans. *Biochem. Pharmacol.* **1963**, *12*, 779−794.
(49) Craig, J. C.; Gruenke, L.; Lee, S. Radiopharmaceuticals, Synthesis of deuterium-labelled chlorpromazine and chlorpromazine metabolites. *J. Labelled Compd. Radiopharm.* **1978**, *15*, 31−40.

https://doi.org/10.1021/acs.joc.1c01407
J. Org. Chem. 2021, 86, 14563−14571